

# STUDYING EFFECT OF ELONGATIONAL VISCOSITY ON THE VELOCITY DISTRIBUTION FOR DRY/WET-SPUN NASCENT HOLLOW FIBER MEMBRANE

Quasy F. Alsahy

Chemical Engineering Department – University of Technology - Iraq

## ABSTRACT

*A study is carried out to investigate the effect of elongational viscosity on the velocity distribution; the mathematical model of the velocity profile of a nascent hollow fiber during membrane formation in the air-gap region was numerically simulated by using Runge-Kutta method (fourth order method). The effect of mass transfer described by a function  $G(C_h^5)$  was studied in two cases: in the first case, mass transfer was constant, in the second when mass transfer was variable. The latter was done by varying with the concentration of solvent in a nascent hollow fiber through the air-gap region. From the calculated results it can be seen that the effect of elongational viscosity in the second case ( $G(C_h^5)$  variable) on velocity distribution of a nascent hollow fiber more closely and clearly than the first case ( $G(C_h^5)$  constant) and the modal calculation values were in a good agreement with the experimental values. An attempt is made to predict the concentration profile of solvent in the moving filament by simultaneously solving the mass and force balance equations, in which the increase in elongational viscosity along the spinning way is mainly due to the hardening process. To prove our hypotheses, hollow fiber membranes were spun from 20:80 polybenzimidazole/polyetherimide dopes with 25.6 wt% solid in N,N-dimethylacetamide using water as the external and internal coagulants.*

## INTRODUCTION

Membrane researchers have focused on the following aspects during hollow fiber spinning in order to obtain hollow fiber membranes with high performance: structure and dimensions of the spinning [1-3]; composition and temperature of the dope solution [4]; the viscosity and the possibility of spinning of the dope [5]; dope extrusion rate [6]; composition, temperature and flow rate of the bore fluid [6,7]; length and humidity of the air gap [6-8]; fiber take-up speed [6,9]; and so on.

The importance of the effect of dope flow rate on morphology and properties of hollow fiber membranes has been gradually paid much attention only since 1985 [6]. Recently, fundamental research has been focus on the effect of shear stress (rate) within the spinneret because it is recognized that the dope rheology does play a very important role in the process of hollow fiber membrane formation [10].

Aptel et al. investigated the effect of dope extrusion rate on properties of polysulfone hollow fiber UF membranes by the dry-jet wet spinning process. They reported that the water

flux of final fibers increased but the rejection decreased when the extrusion rate of spinning dope through the spinneret decreased. They stated that their results could be explained by the reason that an increase in the extension of the polymer chains in the direction of flow was produced with an increase in the shear rate [11].

Besides, Tae and co-workers studied numerical simulation of a hollow-fiber melt spinning process [12]. By considering the changes in inner and outer boundaries, initial dimensions of inner and outer radii were obtained by measuring the dimensions of extrudate swell point using a capturing device and extrudate swell played an important role in determining the initial dimensions of the inner and outer radii. But less effect on the hollow portion at the die swell point and found that the mass throughput rate and take-up velocity increase the spinning temperature decreases, the hollow portion of a spun fiber increases. Sysoev and Alexey investigated a mathematical model and Matlab-5 computer code to study the dynamic response of the hollow fiber membrane probe. The depletion layer formation at the sample/membrane interface is taken into



consideration by the mathematical model for the liquid mobile phase. The method can be applied both for gas and liquid feed streams. With this simulation technique, they studied the concentration profiles in a mobile phase and the flux through the hollow fiber membrane inlet as a function of liquid-phase flow rate [13].

In this study, the mathematical equation of the velocity profile of a nascent hollow fiber during formation in the air gap region was numerically simulated by using Runge-Kutta (fourth order method) in order to find the effects of elongational viscosity of dope solution on the velocity distribution.

### THEORY

Chung and Xu derived the velocity profile equation of a nascent hollow fiber during formation in the air gap region [14]. Its equation was as follows

$$\bar{V}_{h,z} \frac{d\bar{V}_{h,z}}{dZ} = g + \bar{V}_{h,z} \frac{d}{dZ} \left[ \frac{\tau_{z,z}}{\rho_h \bar{V}_{h,z}} \right] - \left[ \frac{2R_o(\rho_a \bar{V}_{h,z} f_o + H_o \sigma_o R'_o)}{\rho_h (R_o^2 - R_i^2)} \right] \quad (1)$$

In Equation (1),  $\bar{V}_{h,z}$  is the average velocity of a nascent hollow fiber over the cross section,  $\sigma_o$  is the surface tension,  $\rho_h$  and  $\rho_a$  are the density of a nascent hollow fiber and ambient air, respectively. The most difficult part of solving Equation (1) is how to express the spinning-line stress ( $\tau_{z,z}$ ) as a function of rheological parameters of a spinning solution during the hardening process, where solvent/non-solvent coagulation occurs simultaneously [15-18]. Han and Segal proposed the following simple equation to relate the elongation stress and viscosity on solvent concentration during the hardening (coagulation) stage [17]:

$$\eta_E(\gamma_E, C_h^s) = F(\gamma_E) G(C_h^s) \quad (2)$$

In this case,  $G(C_h^s)$  may be a complicated function that relates the effects of decreasing solvent concentration, as well as increasing non-solvent concentration on viscosity. Thus, the relationship between ( $\tau_{z,z}$ ) and ( $\eta_E$ ) may be expressed as:

$$\tau_{z,z} \approx 3\eta_E G(C_h^s) \frac{d\bar{V}_{h,z}}{dZ} \quad (3)$$

By substitute equation (3) in equation (1), the following equation is obtained:

$$\bar{V}_{h,z} \frac{d\bar{V}_{h,z}}{dZ} = g + \left( \frac{3\bar{V}_{h,z} \eta_E}{\rho_h} \right) \frac{d}{dZ} \left[ \left( \frac{G(C_h^s)}{\bar{V}_{h,z}} \right) \frac{d\bar{V}_{h,z}}{dZ} \right] - \left[ \frac{2R_o(\rho_a \bar{V}_{h,z} f_o + H_o \sigma_o R'_o)}{\rho_h (R_o^2 - R_i^2)} \right] \quad (4)$$

In order to rewrite equation (4) in the dimensionless form, it is supposed that the complicated function  $G(C_h^s)$  is constant:

$$\frac{d^2 \bar{V}_{h,z}}{dZ^2} - \frac{1}{\bar{V}_{h,z}} \left( \frac{d\bar{V}_{h,z}}{dZ} \right)^2 - \left( \frac{\rho_h \bar{V}_{h,z}}{3\eta_E G(C_h^s)} \right) \frac{d\bar{V}_{h,z}}{dZ} - \left[ \frac{2R_o \rho_a f_o}{3\eta_E G(C_h^s) (R_o^2 - R_i^2)} \right] \bar{V}_{h,z} + \left[ g - \frac{H_o \sigma_o R'_o}{\rho_h (R_o^2 - R_i^2)} \right] \frac{\rho_h}{3\eta_E G(C_h^s)} = 0 \quad (5)$$

Where  $H_o$  is the combined reciprocal radii of the curvatures at the outer skin and it can be expressed as follows [14]:

$$H_o = \frac{1}{R_o [1 + (R'_o)^2]^{\frac{1}{2}}} - \frac{R''_o}{[1 + (R'_o)^2]^{\frac{3}{2}}} \quad (6)$$

Where  $R'_o$  and  $R''_o$  are the first and second derivatives of outer radius of a nascent hollow fiber respectively [14].

Equation (5) is to be solved with the boundary conditions:

$$i) \text{ At } Z = 0, \bar{V}_{h,z} = \bar{V}_{h,0} \quad (7)$$

$$ii) \text{ At } Z = L, \bar{V}_{h,z} = \bar{V}_{h,L} \quad (8)$$

But when it is suppose that the complicated function  $G(C_h^s)$  is variable, Han and Segal proposed the following expression for  $G(C_h^s)$  based solely on their experimental result [17]:

$$G(C_h^s) = 1 + A[C_o - C(Z)] + B[C_o - C(Z)]^2 \quad (9)$$

Where,  $C_o$  is the initial concentration of solvent in the dope solution [Table 1],  $C(Z)$  is the concentration of the solvent in the elongation filament which can be get from experimental



data<sup>[14]</sup>, and constants A and B are empirical constants to be determined. Equation (4) becomes:

$$\frac{d^2 \bar{V}_{h,z}}{dZ^2} - \frac{1}{\bar{V}_{h,z}} \left( \frac{d\bar{V}_{h,z}}{dZ} \right)^2 + \frac{1}{G(C_h^s)} \left( \frac{dG(C_h^s)}{dZ} \right) \left( \frac{d\bar{V}_{h,z}}{dZ} \right) - \frac{\rho_h}{3\eta_E G(C_h^s)} \left[ \bar{V}_{h,z} \left( \frac{d\bar{V}_{h,z}}{dZ} \right) - \bar{V}_{h,z} \left( \frac{2R_o \rho_o f_o}{R_o^2 - R_i^2} \right) - \left( g - \frac{H_o \sigma_o R_o'}{\rho_h (R_o^2 - R_i^2)} \right) \right] = 0 \quad (10)$$

However, in solving equation (10) one has know  $C(Z)$ , the concentration profiles of the solvent in the elongating filament along the spinning way. This necessitates solving a mass balance equation together with equation (10).

Chung and Xu<sup>[14]</sup> derived an equation of mass transfer (solvent) in a nascent hollow fiber as follows:

$$\bar{V}_{h,z} \frac{dC_h^s}{dZ} = -\frac{2R_i K_i}{R_o^2 - R_i^2} (C_h^s - C_b^s) + D_{sp} \frac{d^2 C_h^s}{dZ^2} \quad (11)$$

In equation (11),  $K_i$  is mass transfer coefficient of solvent at the inner interface and is assumed to be constant.  $C_b^s$  represent the average solvent concentration in bore fluid.

We suppose that the concentration profile

within the filament at any position  $Z$ , is a flat and a constant bath concentration, then equation (11) become

$$\bar{V}_{h,z} \frac{dC_h^s}{dZ} = -\frac{2R_i K_i}{R_o^2 - R_i^2} (C_h^s - C_b^s) \quad (12)$$

Equation (10) is to be solved with the boundary conditions given by Equation (7) and Equation (8). Equation (12) is to be solved with the boundary condition:

$$Z = 0, C_h^s = C_0 \quad (13)$$

Solution of the mass balance equation, equation (12), simultaneously with the force balance equation, equation (10), by using Runge-Kutta method (fourth order method), gives the prediction of the fiber velocity and concentration profiles.

## RESULTS AND DISCUSSION

Equation (4) described the velocity profile of a nascent hollow fiber in the air gap region as a function of gravity, mass transfer, surface

tension, drag forces and rheological parameters of spinning solution [14]. By using numerical fourth order Runge-Kutta method, Equation (5), Equation (10) and Equation (12) solved with the boundary conditions given by Equation (7), Equation (8) and Equation (13), to study the effect of elongational viscosity on the velocity distribution of a nascent hollow fiber and to find the amount of solvent removed from filament through the spinning way.

The effect of elongational viscosity ( $\eta_E$ ) on the velocity distribution was studied in two cases. The first case when the magnitude of mass transfer through the spinning process is constant and the second when the magnitude of mass transfer is variable. The effect of mass transfer on velocity distribution was described by a function ( $G(C_h^s)$ ). Equation (2) describe relate the elongational viscosity on solvent concentration during the hardening stage. Where, when the concentration of solvent decrease cause increasing in a function ( $G(C_h^s)$ ), then the elongational viscosity will be increase. As seen in Fig. 1, it is shown that the effect of different values of elongational viscosity on velocity distribution of a nascent hollow fiber in the first case is different, where, the mass transfer is constant [described by a function  $G(C_h^s)$ ][Equation (5)]. It could also been seen that the magnitude of the elongational viscosity increases with a decrease of the velocity distribution and the effect of elongational viscosity ( $\eta_E$ ) appear apparently after a distance of 7 cm from the spinneret hole. It is concluded that the fixation of the solvent concentration in a nascent hollow fiber during the membrane formation affects on the effect of elongational viscosity ( $\eta_E$ ).

In the second case, when the influence of mass transfer is variable, while the empirical equation proposed by Han and Segal was used to describe this variety, in which Equation (9) showed the dependence of a function on the solvent concentration in a filament, where the concentration of solvent decrease during formation in air gap region. As shown in Equation (10), the velocity profile of a nascent hollow fiber for case 2 is described. The effect of different values of elongational viscosity ( $\eta_E$ ) on velocity distribution is discussed in Fig. 2 and it could be seen that the predicted results were more closely than the first case because of the



effect of decreasing in the concentration of solvent in the filament and the effect of

elongational viscosity ( $\eta_E$ ) appear apparently after a distance of 2 cm from the spinneret hole.

Table 2 shows the optimum value of  $G(C_h^s)$ ,  $\sigma_o$  and  $f_o$  which offer a good agreement with the experimental data by using parameter identification procedure. Table 3 summarizes the experimental values of inner diameter ( $D_i$ ) and outer diameter ( $D_o$ ) and the experimental and predicted values of the velocity of a nascent hollow fiber with air gap distance in two cases. Fig.3 gives the resultant concentration profile of solvent in the fiber. It is seen that approximately (92%) of the original concentration of solvent remains in the filament at about a distance 5 cm from the spinneret face. Since  $C(Z)$  can never go below the equilibrium concentration  $C_b$ , estimate the solvent removal with respect to the maximum amount of solvent, which can be removed, is  $[(C(Z) - C_b)/(C_o - C_b)]$ . This quantity is also plotted in Fig.3, and it is seen that when 8% of the original solvent is removed from the fiber, the solvent concentration has moved toward equilibrium by approximately 12%. Then, the percentage of solvent removed from the filament is low. Furthermore, we are considering the average concentration in the filament at any position  $Z$ . As shown in Fig.4, the plots of both experimental and predicted velocity profile with empirical constant A, B and  $K_i$  are compared. A reasonably good fit to the velocity data was obtained with  $4.8 \times 10^4$ ,  $-8.5 \times 10^4$  and  $5.67 \times 10^{-3}$  values of A, B and  $K_i$  respectively.

Table (1) Process parameters and spinning conditions of hollow fibers

Process Parameter	Spinning Condition
Spinning polymer solution	PBI/PEI/DMAc
Polymer concentration (20:80 PBI:PEI)	25.6 wt%
Initial concentration of solvent in dope solution	0.724
Viscosity at 25 °C	6600 cp
Bore fluid	water
Bore fluid rate	0.00417 cm <sup>3</sup> /s
Dope flow rate	0.0142 g/s
External coagulant	water
Range of air-gap	0-30 cm
Take-up velocity	3.33-4.94 cm/s
Density of ambient air	$1.186 \times 10^{-3}$ g/cm <sup>3</sup>
Density of a hollow fiber	1.01 g/cm

Table (2) Parameters identified

$G(C_h^s)$	$\sigma_o$ (dyne cm <sup>-1</sup> )	$f_o$	$F = \sum_i (\bar{V}_{h,z} - \bar{V}_{h,z}^P)^2$
2997	80.9	1.1	0.054

Table (3) Experimental and Prediction Values

Air-Gap Dis. (cm)	$\bar{V}_{h,z}$ (cm/s)	$\bar{V}_{h,z}^P$ Case1 (cm/s)	$\bar{V}_{h,z}^P$ Case2 (cm/s)	$D_o$ (cm)	$D_i$ (cm)
0	3.33	3.33	3.33	0.084	0.040
10	3.47	3.55	3.64	0.082	0.039
20	4.32	4.02	4.17	0.073	0.035
30	4.94	4.94	4.94	0.069	0.033

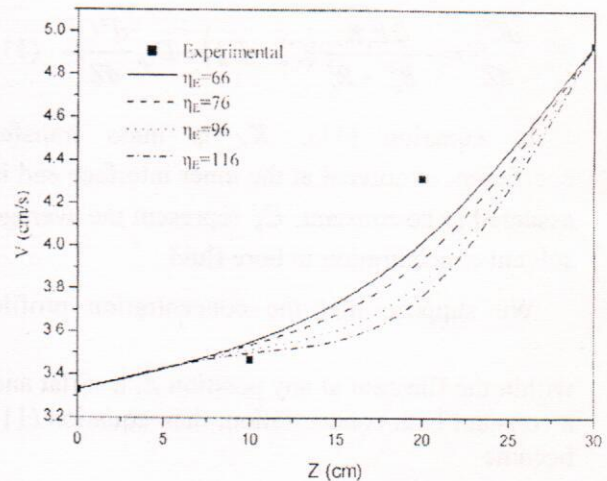


Fig. (1) Influence of elongation viscosity ( $\eta_E$ ) on the velocity distribution in the first case

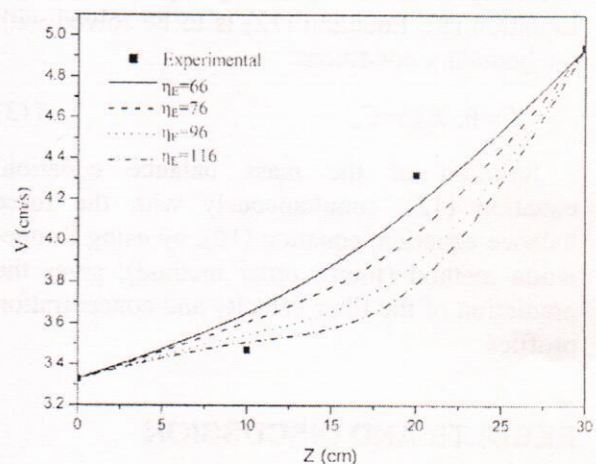


Fig. (2) Influence of elongation viscosity ( $\eta_E$ ) on the velocity distribution in the first case



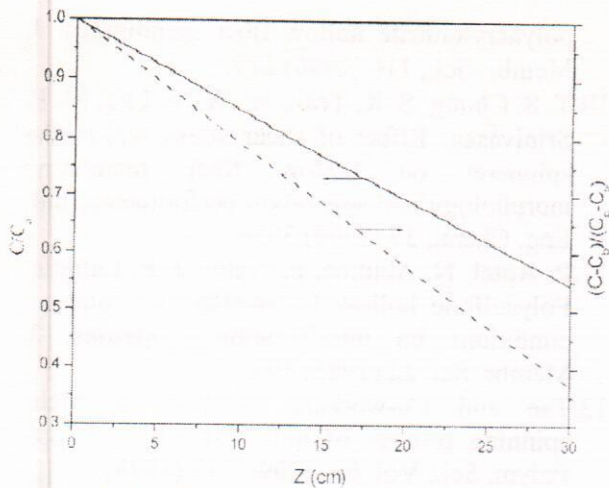


Fig. (3) Predicted concentration profile of solvent (DMAc) in wet/dry-span PB1/PEI fiber

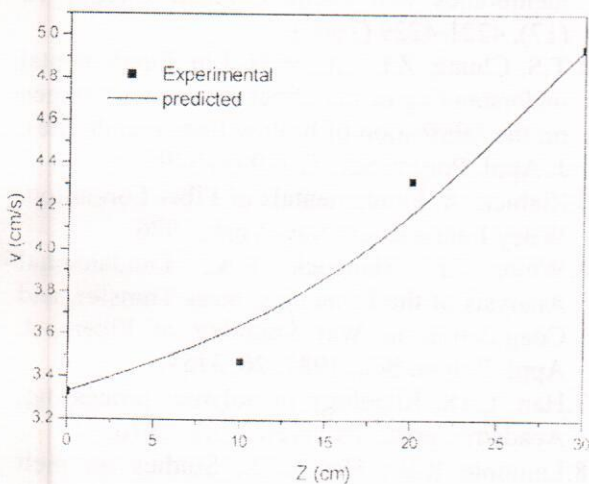


Fig. (4) Compare between prediction and experiment in the second case parameters used for curve fitting:  
 $k_1=5.67 \cdot 10^{-3}$ ;  $A=4.8 \cdot 10^4$ ;  $B=-8.5 \cdot 10^4$

## CONCLUSIONS

Two equations described the velocity and concentration profile of a nascent hollow fiber during formation in the air gap region was solved numerically by using Runge-Kutta (fourth order method) to study the effect of elongational viscosity  $\eta_E$  on velocity distribution of a nascent hollow fiber during formation. In this study the effect of mass transfer was studied in two cases. One was that mass transfer was constant while another was that mass transfer was variable. The effect of mass transfer described by a function ( $G(C_h^s)$ ) on velocity distribution. The effect of

elongational viscosity in the second case on velocity distribution of a nascent hollow fiber more closely and clearly than in the first case. The classical Runge-Kutta fourth order numerical method was most often used because of its simplicity and moderate order.

## ACKNOWLEDGMENT

This study is supported by National Nature Science Foundation of China (No. 20076009).

## NOMENCLATURE

### Symbols

- $C_h^s$  solvent concentration in a nascent hollow fiber (g cm<sup>-3</sup>).
- $C_b^s$  average solvent concentration of bore fluid (gm cm<sup>-3</sup>).
- $D_{sp}$  diffusion coefficient of solvent in a nascent hollow fiber (gm cm<sup>-3</sup>).
- $f_o$  drag coefficient at the external surface of a nascent hollow fiber.
- $F(\gamma_E)$  material function defined [Eq.2].
- $g$  gravitational function (980 cm s<sup>-2</sup>).
- $G(C_h^s)$  material function defined [Eq.2].
- $H_o$  the combined reciprocal radii of the curvatures at the outer skin of the nascent hollow fiber (cm<sup>-1</sup>).
- $K_i$  mass transfer coefficient of solvent at the inner interface (cm s<sup>-1</sup>).
- $L$  air-gap distance (cm).
- $R_i$  inner radius of a nascent hollow fiber (cm).
- $R_o$  outer radius of a nascent hollow fiber (cm).
- $R_o', R_o''$  the first and second derivative of  $R_o$ , with respect to  $Z$ , respectively.

### Greek letters

- $\sigma_o$  surface tension at air and nascent hollow fiber interface (dyne cm<sup>-1</sup>).
- $\gamma_E$  strain rate or rate of elongation (s<sup>-1</sup>).
- $\eta_E$  elongational viscosity.
- $\bar{V}_{h,z}$  average velocity over the cross-section (cm s<sup>-1</sup>).
- $\rho_a$  density of ambient air (g cm<sup>-3</sup>).
- $\rho_h$  density of nascent hollow fiber (g cm<sup>-3</sup>).
- $\tau_{z,z}$  extra stress (dyne cm<sup>-2</sup>).



## REFERENCES

1. Z. Tadmor, C. G. Gogos, Principles of polymer processing, Wiley, New York, 1979, 543pp.
2. J. R. A Pearson, Mechanics of polymer processing, Elsevier, London, 1985, 190 pp.
3. T.S. Chung, S.K. Teoh, W.W.Y. Lau, M. P. Srinivasan. Effect of shear stress within the spinneret on hollow fiber membrane morphology and separation performance. *Ind. Eng. Chem.* 37 (1998) 3930 and the subsequently correction, *Ind. Eng. Chem.* 37 (1998) 4903.
4. S. C. Pesek, W. J. Koros, Aqueous quenched asymmetric polysulfone hollow fibers prepared by dry/wet phase separation, *J. Membr. Sci.* 88 (1994) 1.
5. I. Cabasso, E. Klein, J. K. Smith, Polysulfone hollow fibers. I. Spinning and properties, *J. Appl. Polym. Sci.* 20 (1976) 2377.
6. S.A. Mckelvey, D.T. Clausi, W.J. Koros, A guide to establishing hollow fiber macroscopic properties for membrane applications, *J. Membr. Sci.* 124 (1997) 223.
7. T. S. Chung, S. K. Teoh, X. Hu, Formation of ultrathin high-performance polyethersulfone hollow fiber membranes, *J. Membr. Sci.* 133 (1998) 161.
8. X. Miao, S. Sourirajan, H. Zhang, W.W.Y. Lau, Production of polyethersulfone hollow fiber ultrafiltration membranes, part I, Effects of water (internal coagulant) flow rate and length of air-gap, *Sep. Sci. Technol.* 31 (1996) 141.
9. M. Yang, M. Chou, Effect of post-drawing on the mechanical and mass transfer properties of polyacrylonitrile hollow fiber membranes, *J. Membr. Sci.*, 116 (1996) 279.
10. T. S. Chung, S. K. Teoh, W. W. Y. Lau, M. P. Srinivasan, Effect of shear stress within the spinneret on hollow fiber membrane morphology and separation performance, *Ind. Eng. Chem.*, 37 (1998) 3930.
11. P. Aptel, N. Abidine, F. Ivaldi, J. P. Lafaille, Polysulfone hollow fibers-effect of spinning conditions on ultrafiltration properties, *J. Membr. Sci.* 22 (1985) 199.
12. Tae and Co-workers, Studies on Melt-spinning process of hollow fibers, *J. Appl. Polym. Sci.*, Vol. 68, 1209-1217 (1998).
13. Sysoev, Alexey A., A mathematical model for kinetic study of analyte permeation from both liquid and gas phase through hollow fiber membranes into vacuum, *Anal. Chem.*, 72 (17), 4221-4229 (2000).
14. T.S. Chung, Z.L. Xu, W.H. Lin, Fundamental understanding of the effect of air gap distance on the fabrication of hollow fiber membranes, *J. Appl. Polym. Sci.* 72 (1999) 379.
15. Ziabick, A. Fundamentals of Fiber Formation, Wiley Interscience: New York, 1976.
16. White J.L. Hancock T.A., Fundamental Analysis of the Dynamics, mass Transfer, and Coagulation in Wet Spinning of Fibers, *J. Appl. Polym. Sci.*, 1981, 26, 3157.
17. Han, C.D., Rheology in polymer processing; Academic press, Inc: New York, 1976.
18. Lamonte R.R.; Han C.D., Studies on melt spinning. II. Analysis of the deformation and heat transfer processes, *J. Appl. Polym. Sci.*, 1972, 16, 3285.